ADVANCES IN ATMOSPHERIC SCIENCES, VOL. 30, NO. 2, 2013, 330–340

The Influence of Regional SSTs on the Interdecadal Shift of the East Asian Summer Monsoon

FU Jianjian[1] (付建建) and LI Shuanglin*[1,2] (李双林)

[1] *Climate Changes Research Center and Nansen-Zhu International Research Centre, Institute of Atmospheric Physics, Chinese Academy of Sciences, Beijing* 100029

[2] *Key Laboratory of Regional Climate-Environment for East Asia, Institute of Atmospheric Physics, Chinese Academy of Sciences, Beijing* 100029

(Received 20 March 2012; revised 29 May 2012)

ABSTRACT

East Asia has experienced a significant interdecadal climate shift since the late 1970s. This shift was accompanied by a decadal change of global SST. Previous studies have suggested that the decadal shift of global SST background status played a substantial role in such a climatic shift. However, the individual roles of different regional SSTs remain unclear. In this study, we investigated these roles using ensemble experiments of an atmospheric general circulation model, GFDL (Geophysical Fluid Dynamics Laboratory) AM2. Two kinds of ensembles were performed. The first was a control ensemble in which the model was driven with the observed climatological SSTs. The second was an experimental ensemble in which the model was driven with the observed climatological SSTs plus interdecadal SST background shifts in separate ocean regions. The results suggest that the SST shift in the tropics exerted more important influence than those in the extratropics, although the latter contribute to the shift modestly. The variations of summer monsoonal circulation systems, including the South Asian High, the West Pacific Subtropical High, and the lower-level air flow, were analyzed. The results show that, in comparison with those induced by extratropical SSTs, the shifts induced by tropical SSTs bear more similarity to the observations and to the simulations with global SSTs prescribed. In particular, the observed SST shift in the tropical Pacific Ocean, rather than the Indian Ocean, contributed significantly to the shift of East Asian summer monsoon since the 1970s.

Key words: East Asian summer monsoon, interdecadal shift, SST, AGCM

Citation: Fu, J. J., and S. L. Li, 2013: The influence of regional SSTs on the interdecadal shift of the East Asian summer monsoon. *Adv. Atmos. Sci.*, **30**(2), 330–340, doi: 10.1007/s00376-012-2062-3.

1. Introduction

The East Asian summer monsoon (EASM) has undergone major interdecadal weakening since the late 1970s (Huang, 2001; Wang, 2001). This weakening has been accompanied by an interdecadal change of global SST, including warming in the tropical Indian Ocean (Hoerling et al., 2004) and in the tropical eastern Pacific (e.g., Zhang et al., 1997), but cooling in the central North Pacific (Fig. 1). The role of the interdecadal shift of the SST in the EASM shift has been the subject of much investigation. Based on observational analyses, Hu (1997) demonstrated that the interdecadal variability of the East Asia summer climate is largely controlled by the interdecadal variability of SSTs in the tropical Indian and western Pacific oceans. In contrast, Huang (2001) and Gong and Ho (2002) suggested that the ENSO-like decadal warming in the tropical central-eastern Pacific may be the cause of the EASM shift. Using the EOF method and regression analysis, Zhang et al. (2007) showed that the interdecadal variations of summer precipitation over eastern China are modulated by the temporal evolution of the Pacific Decadal Oscillation (PDO), a basin-scale interdecadal SST variability mode that occurs across the whole northern Pacific Ocean.

The SST influence hinted at the observational studies has been further studied in climate modeling ex-

*Corresponding author: LI Shuanglin, shuanglin.li@mail.iap.ac.cn

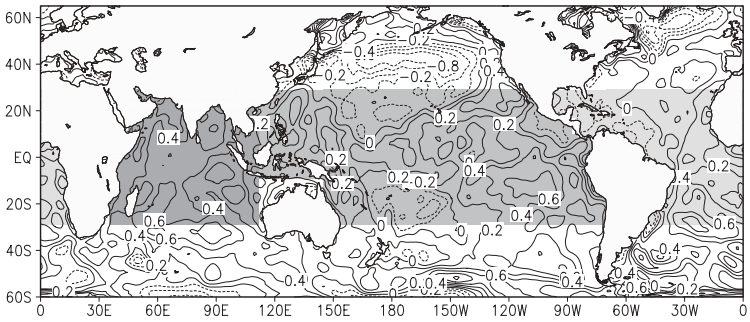

Fig. 1. July–August mean difference in SST between the periods 1979–1998 and 1950–1969. Units: °C. Shadings indicate different tropical regions with SST background state modified. See the context.

periments. Fu et al. (2009) forced an atmospheric general circulation model (AGCM), Geophysical Fluid Dynamics Laboratory (GFDL) AM2, with two different SST climatological states, one prior to the shift and another following the shift. Their results suggest that the decadal shift of global SST basic state has played a substantial role. Consistent with this conclusion, Zeng et al. (2007) forced another AGCM, National Centers for Atmosphere Research's CAM3, with observed historical SST evolution, and their results suggest that the global SST shift, particularly the recent warming in the North Indian Ocean and the South China Sea, may be responsible for the EASM shift in part. Also, Li et al. (2008a) forced GFDL AM2 with historical SSTs as well as chemical forcing and their results showed that the historical SSTs, particularly in the tropical Indian and western Pacific oceans, can account for the EASM shift. Consistent with this analysis, Zhou et al. (2009) used several AGCMs to study the roles of Indian and western Pacific ocean SSTs in the interdecadal shift of the Western Pacific Subtropical High (anticyclone, WPSH), an important subsystem of the EASM. Their results showed that the SST can explain the interdecadal westward and southward shift of the anticyclone. In contrast, Li et al. (2008b) gave special attention to the role of the tropical Indian Ocean. They conducted ensemble experiments in five AGCMs by prescribing an idealized tropical Indian Ocean warming, and they illustrated that the Indian Ocean warming intensifies the southwesterly winds toward East China as well as the South Asian High (SAH), subsequently enhancing the EASM. Therefore, the interdecadal warming of the tropical Indian Ocean alone cannot explain the observed interdecadal weakening of the EASM. These analyses suggest uncertainty regarding the influences of different regional SSTs, in spite of a consensus regarding the contribution of global SST in general. It is therefore compelling to ask: What are the roles of different regional SST changes like those in the tropical Indian and Pacific oceans? This issue constitutes the primary motivation of the present study. Like Fu et al. (2009), we conducted sensitive experiments in GFDL AM2 by prescribing different basic SST states.

The remainder of the paper is organized as follows. Section 2 describes the datasets, model, and experimental design. Section 3 validates the model's simulations on the EASM. The model results concerning the influence of regional SST variations on the EASM interdecadal shift are presented in section 4. A summary and concluding remarks are given in the last section.

2. Datasets, model, and experimental design

2.1 *Observational datasets*

The observational SST dataset was acquired from the Global Integrated Sea Surface Temperature and sea ice dataset (GISST) (Rayner et al., 1996). The observational atmospheric circulation datasets were provided by the National Centers for Environmental Prediction-National Center for Atmosphere Research (NCEP-NCAR) reanalysis (Kalnay et al., 1996) for the period 1950–1998 and the ECMWF (European Center for Medium-Range Weather Forecasts) 40-year reanalysis (ERA40) (Upplal et al., 2004) for the period 1958–1998. These datasets are on regular grids with a horizontal resolution of 2.5°×2.5°. The variables included geopotential heights at 100 hPa, 500 hPa, and 850 hPa, and horizontal winds field at 850 hPa. In view of the poor quality of observations prior to 1979 in the Southern Hemisphere in the NCEP-NCAR reanalysis (Renwick, 2002) and the short record length of the ERA40, we used both sets of reanalysis datasets for validation.

Monthly global land precipitation obtained from the Climate Research Unit (CRU), University of East Anglia (Mitchell and Jones, 2005) was used; this data covered a longer period, 1900–2002, and used a 0.5°×0.5° grid resolution. Because no global rainfall dataset was available, the CMAP (Climate Predic-

tion Center Merged Analysis of Precipitation) global monthly rainfall dataset (Xie and Arkin, 1996) starting from 1979 was used to verify the model's rainfall climatology. These datasets were used to compare our simulation results with observed East Asian regional rainfall.

In view of the aforementioned shift, two separate periods, 1979–1998 and 1950–1969, were selected as two phases of interdecadal variations of the EASM. The primary considerations were the following. (1) No agreement has been reached regarding the first exact year of the shift. Therefore, an earlier period, 1950–1969, was used to represent the first phase to avoid the controversy about the turning point. (2) The two periods were not only within the two distinct EASM phases but also had the same time length of 20 years. This time span was convenient for comparison. (3) A different interdecadal shift of the EASM may have occurred around the year 1999 (Si et al., 2009; Zhu et al., 2010). So the period 1979–1998 was the longest period available to represent the EASM phase after the late 1970s. (4) Most importantly, the results remained nearly unchanged when the 20-year temporal window was shifted slightly within the period 1950–1976 for the first phase.

2.2 *GFDL AM2 and experimental design*

GFDL AM2 was used for the present study, and a detailed description of the model can be found in GAMT (2004). The experimental design was as follows. Ensemble experiments were used, and two kinds of ensembles were performed. The first was a control ensemble, in which the model was driven with the observed global climatological monthly SST calculated as the mean during the period 1950–1969 (referred to as period one: P1). The second was a SST shift ensemble, in which the model was driven with the climatological monthly SST plus the interdecadal SST shift (background status shift) over the separate ocean regions. The shifted SST anomalies were calculated as the difference of averaged SST during the period 1979–1998 (referred to as period two: P2) minus those during P1 (Fig. 1). For the second experiment, a total of seven sets of ensembles were performed; each of them corresponded to shifted global SST (referred to as global ocean global atmosphere: GOGA) or in different ocean regions or their combination, including the whole tropics (i.e., 30°S–30°N, the TOGA run), the extratropical (i.e., 30°–55°N, 30°–55°S, the EXTRA run). The following divisions were limited to a northern boundary of 55°N and a southern boundary to 55°S to exclude the potential involvement of sea ice: the tropical Indian Ocean (TIOGA run), the tropical Pacific (TPOGA run), the tropical Atlantic (TAOGA run), and the combined tropical Pacific and Atlantic (TPAOGA run). In other words, in the second ensemble the climatological SST in each of the seven regions was the mean during P2 but was replaced with the mean during P1 elsewhere. A smoothing process was applied to the boundaries of the two kinds of SST climatology to remove the impact of the additional SST gradient. All of the experiments are summarized in Table 1. The difference of modeled climate between the SST shift ensembles minus the control ensemble represents the impact of the SST basic-state shift in different regions.

Table 1. Summary of numerical experiments.

For short	Full name	Number of ensembles	Experimental design
CTL	Control ensemble	2	AGCM is forced by observed climatological monthly SST, which is calculated as the mean through 1950–1969.
GOGA	Global SST forcing	2	As CTL, but the climatology is calculated as the mean through 1979–1998.
TOGA	Tropical SST forcing	2	As GOGA, but the 1979-1998 climatology is just used in the tropics (30°S–30°N).
TIOGA	Tropical Indian ocean SST forcing	2	As TOGA, the 1979–1998 climatology is just used in the tropical Indian ocean.
TPAOGA	Tropical Pacific and Atlantic SST forcing	2	As TOGA, but the 1979–1998 climatology is used just in the tropical Pacific and Atlantic.
TPOGA	Tropical Pacific SST forcing	2	As TOGA, but the 1979–1998 climatology is just used in the tropical Pacific.
TAOGA	Tropical Atlantic SST forcing	2	As TOGA, but the 1979–1998 climatology is just used in the tropical Atlantic.
EXTRA	Extratropical SST forcing	2	As CTL, but the 1979–1998 climatological SST is used in the extratropical oceans (30°–55°N, 30°–55°S).

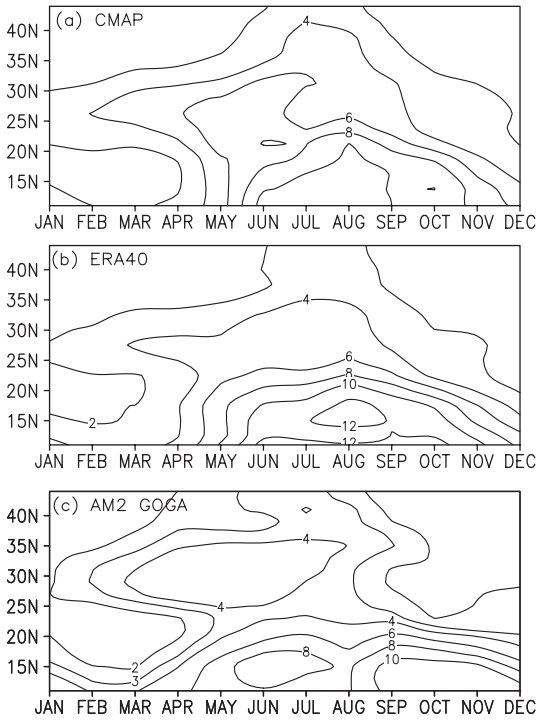

Fig. 2. A comparison of seasonal march of regional zonal-averaged (105°–130°E) rainfall over East Asia in (a) CMAP and (b) ERA40 with that in (c) AM2 GOGA run. Units: mm d^{-1}.

Each ensemble comprised two 25-year runs. The two runs in each ensemble were the same except for a slightly different starting time. The first year in each run was discarded as the model's spin-up period, and thus a total of 48 model years were available for each ensemble. Because the oceanic forcing was the climatological monthly SST, the resulting ensemble had 48 members, each of which was integrated for one year.

3. Validation of the EASM modeled in AM2

Although Fu et al. (2009) showed that AM2 captures the basic aspects of the EASM, a more comprehensive validation of the model's ability in simulating the EASM was conducted in this study. Figure 2 shows the seasonal–latitudinal evolution of climatological monthly precipitation longitudinally averaged between 105°E and 130°E. In this study, the climatology is defined as the mean during P2. The evolution in the three panels bears a considerable consistency, although the rainfall in the model exhibits a northward shift of 2°–3° during summer. For example, during late winter (January to March), the primary rainfall bands were located in the tropical western Pacific, and correspondingly, a rainfall minimum occurred in the subtropics, 10°–20°N. After April, the rainfall increased in the subtropics, which corresponded to a seasonal northward movement of the climatological rainband. In June, rainfall increased significantly near 30°N, corresponding to the onset of the meiyu (baiu in Japanese, changma in Korean) front. The rainfall band reached the northernmost position during midsummer (August). By the end of August, the monsoonal rainfall band retreated to the south. By October, the rainfall band shifted to the south, and the summer monsoon made way for the winter monsoon. These results reflect the fact that the model captured the seasonal march of the EASM. In addition, an abrupt northward jump of the rainfall band occurred from late spring to early summer, which was represented by the acute shift of contours. This means that the model reproduced the sudden northward transition of summer monsoonal rainfall, one significant feature of the EASM (e.g., Lau and Li, 1984).

In addition to rainfall, researchers defined various indices to quantify the activity of the EASM. For this purpose, we used an EASM index (EASMI) proposed by Han and Wang (2007). This EASMI was based on the South Asian Summer Monsoon Index proposed by Webster and Yang (1992) but was modified for EASM. In detail, the index is defined as the normalized zonal wind difference between 850 hPa and 200 hPa averaged over 20°–40°N and 110°–140°E. In addition, we compared two additional indices, the SAH index (SAHI) and the WPSH index (WPSHI), which were used to quantify the activities of the SAH and the WPSH, two primary subsystems of the EASM. The WPSHI is a zonal index describing the seasonal march of the WPSH (adopted from Lu, 2002), defined as the anomalies of geopotential heights at 850hPa averaged over a specified region (30°–40°N, 120°–150°E) at the northern edge of the WPSH. The SAHI was defined as the averaged 100 hPa geopotential heights over the domain (15°–30°N, 70°–130°E), according to Yang et al. (2007).

Figure 3 shows a comparison of the climatological monthly evolution of the EASMI, the WPSHI, and the SAHI. All the three indices simulated in AM2 were consistent with those derived from the two reanalyses. For example, the three indices exhibited similar seasonal evolutions and reached their maxima and/or minima in July–August; however, the values in the model were somewhat smaller (Fig. 3c). The smaller values can be attributed to the model's bias to the decreased geopotential heights in the AM2 simulation (Fu et al., 2009). These validations are consistent with rainband evolutions (Fig. 2), and again they suggest that the AM2 model simulates the EASM realistically.

The rainfall in the Yangtze River valley (YRV) and North China (NC) are governed by the EASM. Follow-

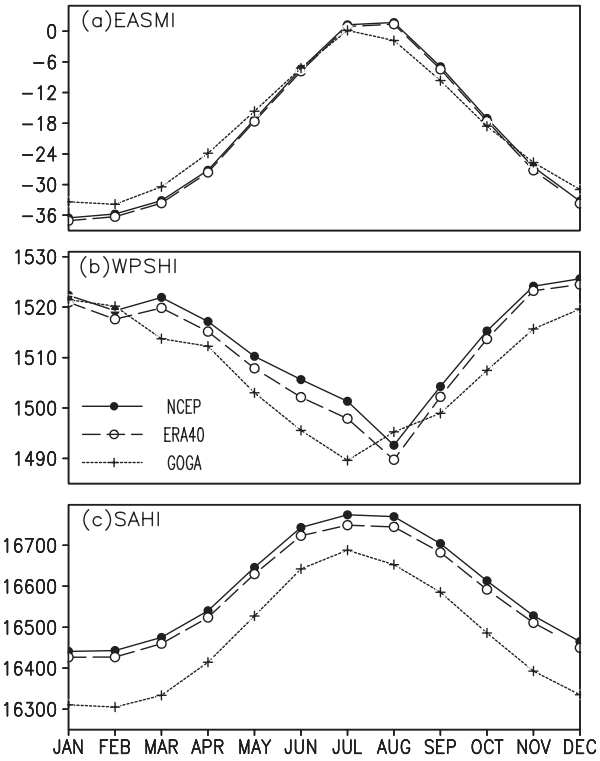

Fig. 3. A comparison of seasonal evolution of (a) EASMI, (b) WPSHI and (c) SAHI in several different datasets. The long dashed lines with circle represent the ERA40 reanalysis, the solid lines with filled dot represent the NCEP-NCAR reanalysis, and the dotted lines with plus sign indicate the AM2 GOGA run. All the indices in both the reanalyses are calculated for the period 1979–98 (P2).

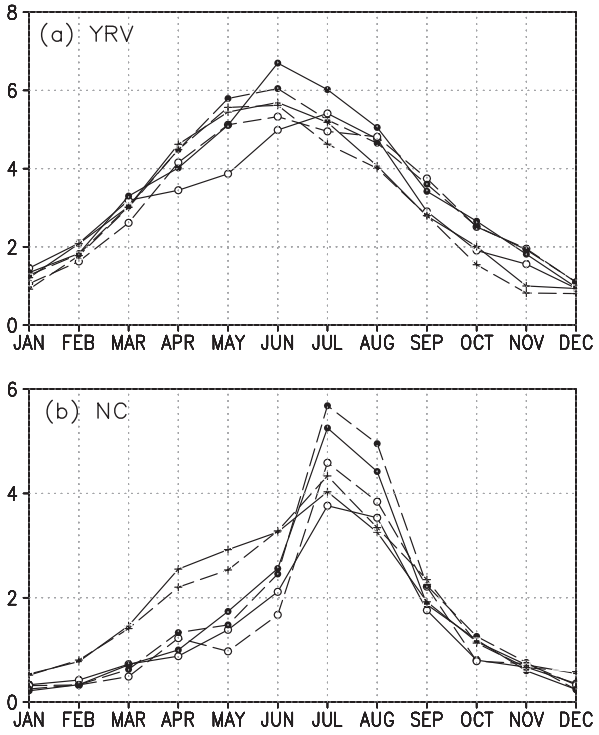

Fig. 4. A comparison of climatological seasonal rainfall evolution in (a) the Yangtze River valley (YRV) and (b) North China (NC) for the two different periods, P1 and P2, in several datasets. Circle indicates the ERA40, filled dot indicates the CRU dataset, and plus sign is for AM2 simulations. Solid and dashed lines indicate the P2 and P1 periods for the observed dataset, and the GOGA and control ensemble in the model experiments, respectively. Units: mm d^{-1}.

ing Li et al. (2008a), we used precipitation indices in these two geographical areas to further evaluate the modeled EASM. Figure 4 shows a comparison of climatological monthly precipitation indices defined as the mean over the YRV (27°–32°N, 105°–122°E) and NC (33°–42°N, 110°–125°E), respectively. The features of climatological rainfall exhibited in Fig. 4 are the same as those shown in Fig. 2. Along with seasonal march, the precipitation in these two areas increased beginning from late spring and reached their maxima during summer. After October, summer monsoonal rainfall decreases swiftly and makes way for the winter monsoon. When period P1 was used to calculate the climatological mean, a similar seasonality was observed (dashed lines in Fig. 4). Compared with P1, the summer rainfall increased in the YRV (Fig. 4a) but decreased in NC (Fig. 4b) during P2 (solid lines), suggesting not a seasonality shift but rather a magnitude shift in the two periods for the two areas. This bears considerable consistency with the observation data (CRU) and the ERA40 reanalysis. Moreover, the observed dipolar pattern in East China (less rainfall in the YRV but more rainfall in NC in P1) in May, June, and other months was well captured by the model. Thus, the interdecadal shift in the context of the global SST basic state can explain not only the summer precipitation shift but also the shifts in other months. In other words, the observed interdecadal rainfall shift can be attributed to the global SST shift to a considerable extent. Thus, in addition to confirming the results of Fu et al. (2009), the present analyses further demonstrate that the AM2 captures the observation characteristics considerably realistically.

4. The impact of regional SSTs

Corresponding to the weakening of the EASM, significant interdecadal changes in large-scale atmospheric circulation have been reported (Hu, 1997). The responses modeled here are believable only provided that the modeled atmospheric circulation re-

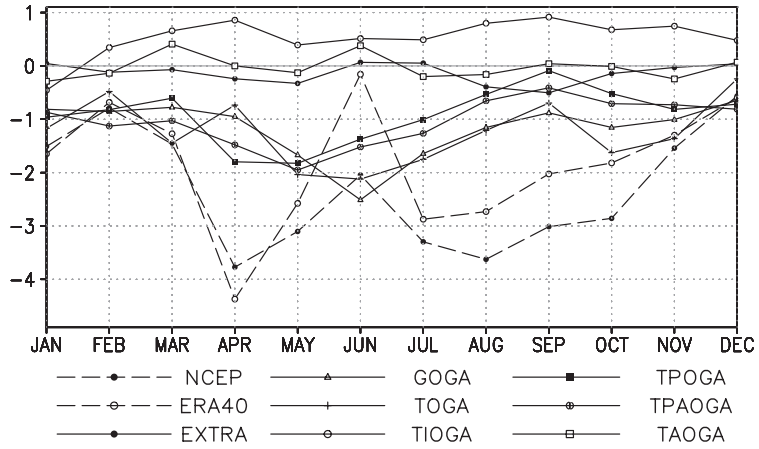

Fig. 5. A comparison of the EASMI difference in P2 minus P1 with the AM2 simulated responses to different regional SST shifts.

sponses capture the primary features of the observations. Li et al. (2008b) and Chen et al. (2010) revealed that the interdecadal warming in the tropical Indian Ocean enhances the EASM. What are the influences of the other regional SSTs? To answer this question, the modeled responses to the SST basic-state shift in different regional oceans were evaluated. First, we compared the combined features of modeled large-scale circulation using the EASMI. Figure 5 shows seasonal evolution of the modeled EASMI response (solid lines) and the observed shift between P2 and P1 from both the reanalyses (dash lines). Except for TIOGA, TAOGA and EXTRA, the response values in the remaining experiments were negative and in agreement with the observed shift. This result indicates that, except for the tropical Indian Ocean and the Atlantic Ocean, the tropical SST shift elsewhere contributed to the interdecadal weakening of the EASMI. Again, the tropical Pacific SST played a dominant role. Nonetheless, these comparisons suggest that tropical SST shift, especially in the tropical Pacific, favored a weakening EASM and thus may account for the observed interdecadal shift of the EASM. In the following section, we report the comparison of the modeled and observed shifts in several key subsystems of EASM.

4.1 *West Pacific subtropical high*

Figure 6 displays a comparison of the July–August mean 500-hPa geopotential height responses with the observed shift, which was used to illustrate the activity of the WPSH. In the reanalyses (Figs. 6h, i), significantly positive anomalies emerged throughout the tropics. Except for the EXTRA case, positive responses were seen in the other experiments. This suggests that the SST shifts in all of the tropical regions contributed to the interdecadal intensification of WPSH; this result is consistent with a previous study (Zhou et al., 2009). These features can also be seen in the modeled and observed WPSHI (Fig. 7). The observed WPSHI shift values in summer were obviously positive, indicating an interdecadal enhancement of WPSHI from P1 to P2. Although the modeled WPSHI responses were positive in nearly all of the experiments, the difference in the impacts of the different tropical regions can be seen in their spatial patterns. In the reanalyses, east to 120°E there was a dipolar anomaly with positive values south to 30°N but negative values in the north. In particular, greater positive values were located at the western rim of the climatological WPSH, indicating an interdecadal westward stretch and southward shift of the WPSH, as revealed in previous studies (e.g., Hu, 1997; Ding et al., 2008). Among all of our experiments, only GOGA, TOGA, TPOGA, and TPAOGA yielded dipolar responses (Figs. 6a, b, d and f), while the TIOGA or EXTRA run reproduced only the northern or southern lobe (Figs. 6c, g). These results suggest that the SST shift in the tropical Pacific, rather than the Indian Ocean or the extratropical oceans, played the dominant role in modulating the observed WPSH shift.

4.2 *The South Asian High*

Figure 8 displays a comparison of the July–August mean 100-hPa geopotential heights to illustrate the activity of the SAH. Here, the shift in ERA40 was calculated as the mean difference in the period of 1979–98 minus that of 1963–77 (Fu and Li, 2012). Positive anomalies occurred in South Asia and Southeast Asia along with identifiable negative anomalies in northeastern Asia in the GOGA, TOGA, TPOGA, and TPAOGA simulation runs (Figs. 8a, b, d, and f), conforming to the observed pattern (Figs. 8h, i). This

means that the global SSTA, particularly in the tropical Pacific or the combined Pacific and Atlantic Ocean, contributed to the observed shift of the SAH. However, no significant responses emerged around the summer climatological location of the SAH (Fig. 8e). Therefore, the role of the tropical Atlantic Ocean SST was minimal. In addition, no significant response can be seen in Figs. 8c and h, meaning that the SST shift in the tropical Indian Ocean or the extratropical Ocean did not substantially contribute to the observed shift of SAH. Interestingly, the response (Fig. 8c) appears as a Gill-type mode, which is reasonable because such a response is a common feature of the atmospheric response to warming in the tropical Indian Ocean (Li et al., 2008b). These SAH response features are also seen in the SAHI (Fig. 9). Visually, the SAHIs in summer in the GOGA, TOGA, TPOGA, and TPAOGA simulation runs were evidently positive and were all statistically significant at the 95% level in June, July, and August, consistent with the observations (Zhang et al., 2000). In comparison, the SAHIs in the EXTRA, TIOGA, and TAOGA runs were negative or neutral (Fig. 8).

4.3 *Subtropical low-level southerly air flow*

The subtropical low-level southerly air-flow transports a large amount of water vapor from the Indian Ocean, the South China Sea, and the western subtropical Pacific to East Asia, and plays a dominant role in modulating summer rainfall in China. The decadal shift of wind fields at 850 hPa displayed a significant northerly anomaly along coastal eastern China in the reanalyses (Figs. 10h and i). The observed shift was simulated in the AM2 when forced with the global SST shift (Fig. 10a). When comparing individual contributions from the tropical and extratropical SSTs, the tropical SST explains a large fraction of the tropical air-flow shift but only a small fraction of the extratropical air-flow shift (Fig. 10b). In comparison, the extratropical northerly anomaly can be primarily attributed to the extratropical SST (Fig. 10g). Furthermore, a comparison of the individual tropical regional

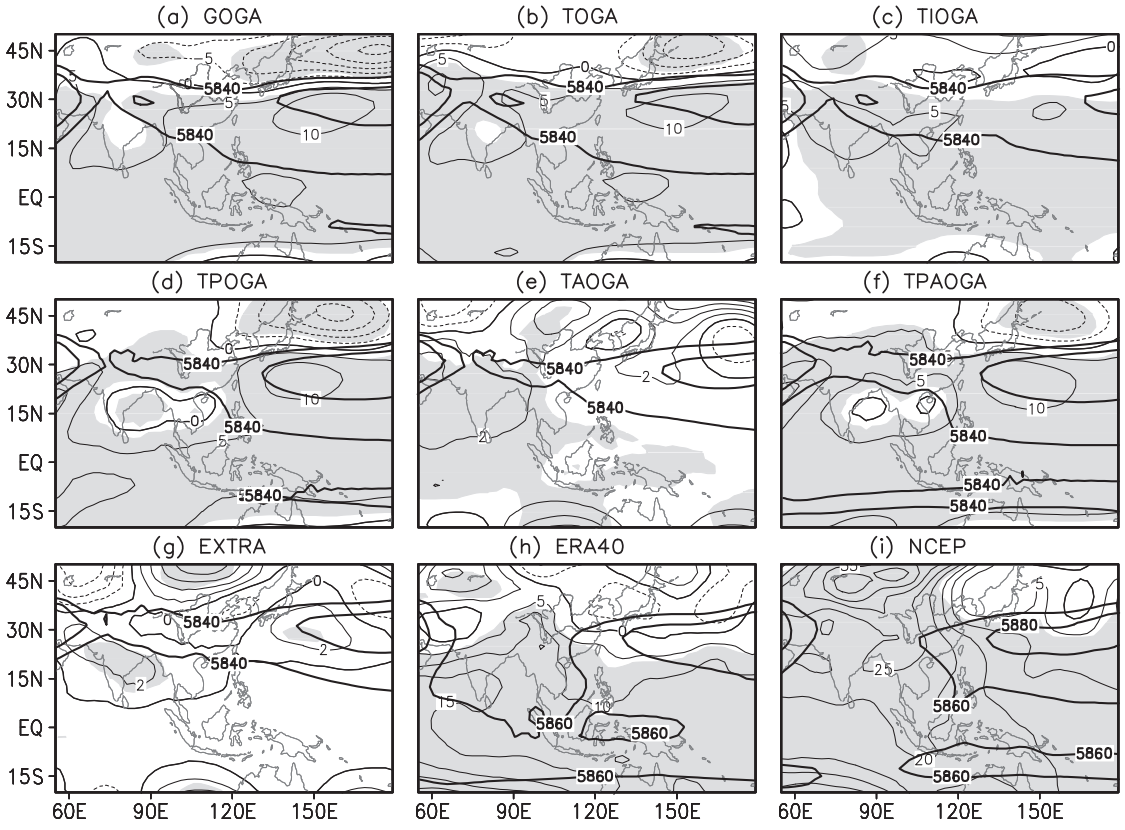

Fig. 6. A comparison of AGCM-modeled summer 500-hPa geopotential height responses (black contours) to different regional SST shift (a–g) with the observed shift in the two reanalyses, ERA40 and the NCEP-NCAR (i, j). Units: gpm. The shading indicates significance at the level of 90%. Climatological characteristic contours, 5840 and 5860, are overlapped additionally to shed light on the impact on the activity of the western Pacific subtropical high. Units: gpm.

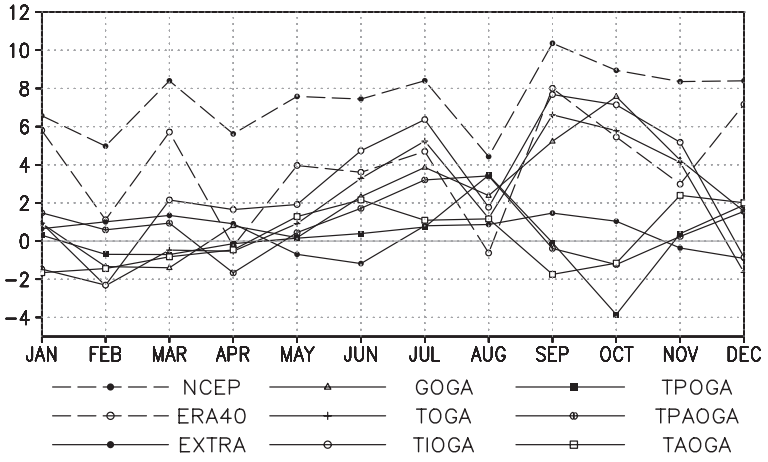

Fig. 7. Same as Fig. 5, but for WPSHI.

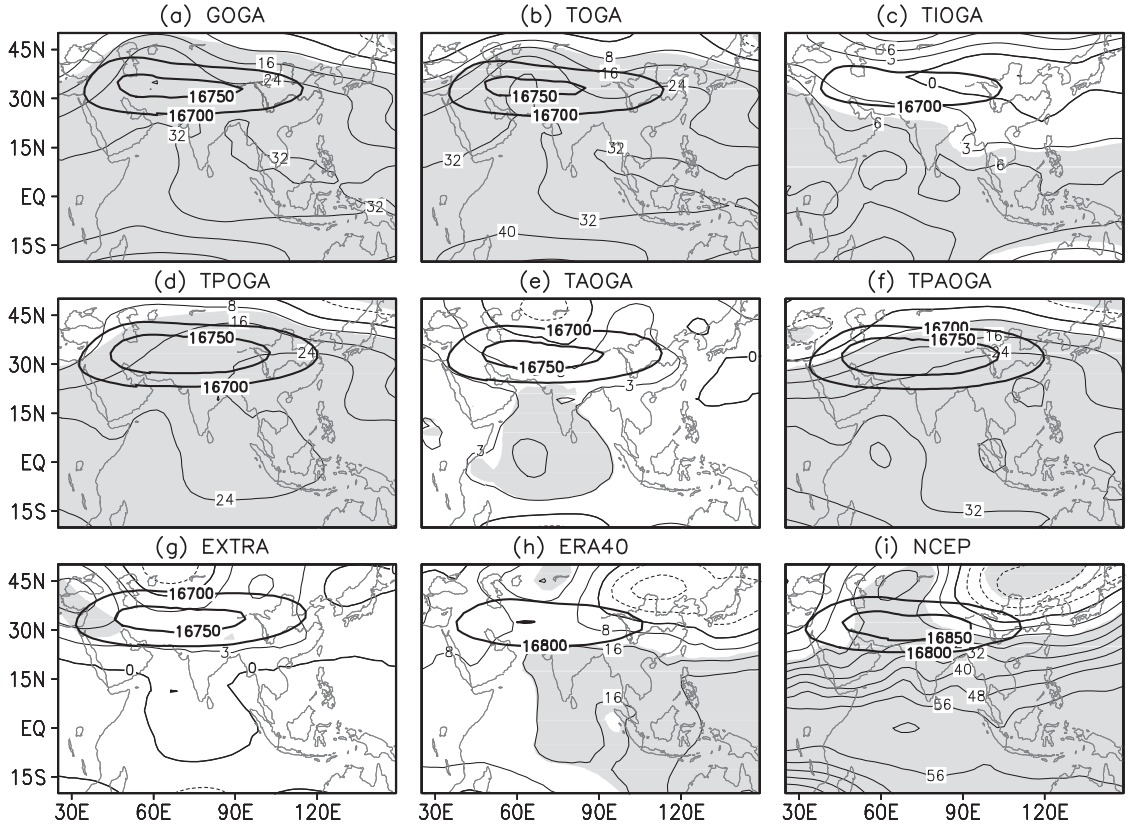

Fig. 8. Same as Fig. 6, but for 100-hPa geopotential height.

SSTs inducing the East Asian northerly anomaly revealed that the role of the tropical Pacific SST was dominant (Fig. 10d), while the role of the tropical Atlantic SST was limited (Fig. 10e). The tropical Indian Ocean SST induced a significant, intensified southwesterly response in South China along the western rim of the WPSH, in contrast to the observations. Such a response enhanced the monsoonal flow rather than weakened the summer monsoonal flow (Fig. 10c) (Li et al., 2008b). These analyses suggest that the SST variations in the tropical Pacific and Atlantic oceans contributed to the observed tropical low-level air-flow shift, while the extratropical SST shift appeared more important for the anomalous northerly flow in East Asia. Thus, the overlapped effects of SSTs in the tropical Pacific and Atlantic oceans with the extratrop-

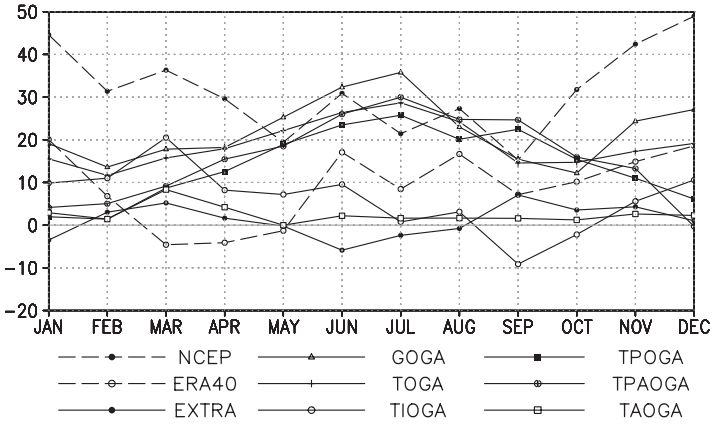

Fig. 9. Same as Fig. 5, but for SAHI.

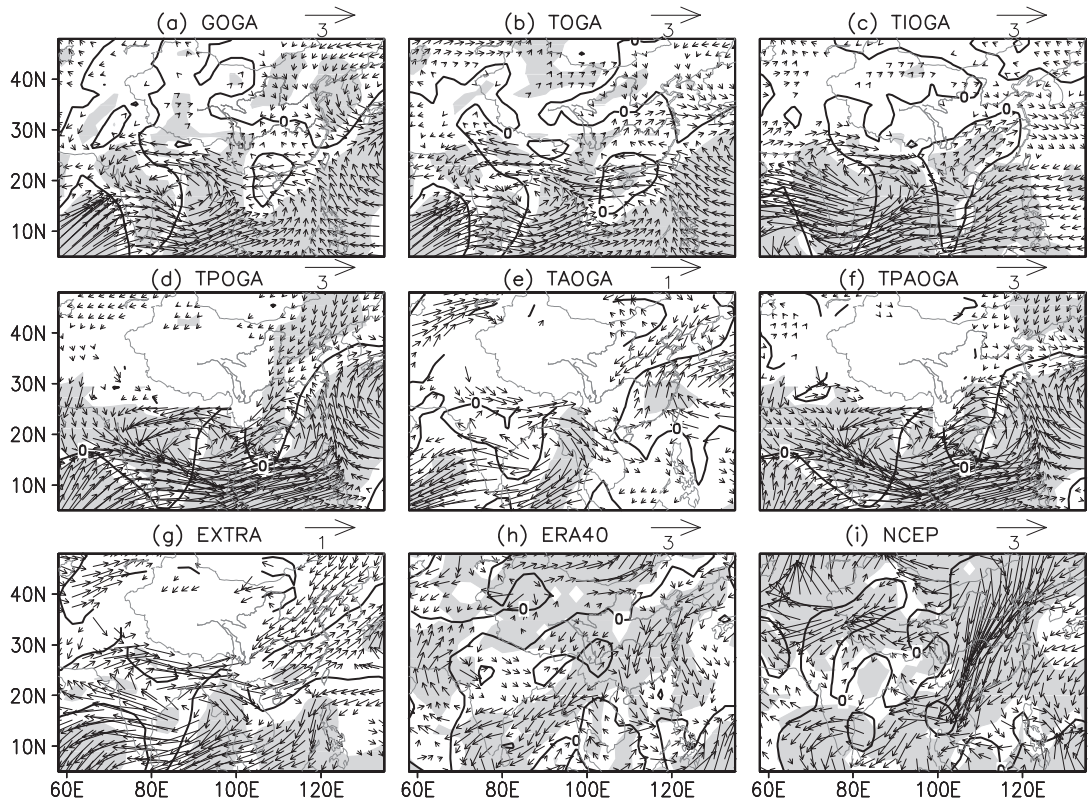

Fig. 10. Same as Fig. 6, but for 850-hPa wind field. Units: m s^{-1}. The shading indicates significance at the level of 90%. The black contour represents the nodal line of meridional wind component.

ics explain the observed low-level air-flow shift. Also, their combination overwhelmed an opposite effect from the tropical Indian Ocean.

5. Discussion and conclusions

In this study, we extended a previous study (i.e., Fu et al., 2009), in which the global SST shift was found to account for the interdecadal shift of the EASM since the late 1970s. We compared individual contributions of regional SSTs by conducting AGCM experiments using GFDL AM2. The primary findings are as follows. (1) The SST shift in the tropical and extratropical oceans both contributed to the interdecadal shift of the EASM, but their roles were not equal. (2) The tropical SST shift explains a larger fraction of the observed EASM shift, including the lower-level monsoonal wind weakening in Southeast China, while the

extratropical SST explains a larger fraction of anomalous lower-level northerly in Northeast Asia and North China. (3) As far as the different tropical regional SSTs are concerned, the tropical Pacific plays the dominant role; the tropical Pacific SST overwhelms the effects from the tropical Indian Ocean. The latter may exert an effect opposite the observed shift. In comparison, the role of the tropical Atlantic is minor, albeit positive.

Our conclusion, which emphasizes the importance of tropical Pacific SST, is consistent with previous observational studies (e.g., Huang, 2001; Gong and Ho, 2002). In addition, our modeling results regarding the Indian Ocean are consistent with those of Li et al. (2008b), in which a comprehensive study was done by forcing five AGCMs with idealized tropical Indian Ocean warming. However, the present result is somewhat different from several previous simulations (e.g., Li et al., 2008a; Zhou et al., 2009; Zeng et al., 2010) and observational analyses as well (e.g., Hu, 1997), which emphasized the combined effect of the tropical Indian and western Pacific oceans, although the combined effect of global SST shift is in agreement. In view of the strong interaction between the tropical Indian and Pacific oceans, the present results focus on the influence of tropical Pacific Ocean and show that the tropical Indian Ocean offsets the influence of the tropical Pacific Ocean to some extent.

There are some weaknesses in this study. First, the SSTs addressed here include only those from the change of background status; they exclude those from transient SST changes. How this influences the present results is unclear. Forcing the AGCM with historical evolving SSTs rather than the SST climatological status shift was helpful in solving this issue. Second, we only investigated the contributions of SSTs. It is well known that not all of the observed variances can be explained by SSTs. Other factors like winter and spring snow cover over the Tibetan Plateau may also play a role (Ding et al., 2009). Yang and Lau (1998) reported that winter–spring warm SST anomalies increased soil moisture in the Asian continent and indirectly weakened the following EASM. Third, we only studied the one-way influence of SSTs on the atmosphere; we did not consider the atmospheric feedback on SSTs. It will be useful to conduct similar studies with coupled climate system models. Finally, two components of the observed SST variation, natural fluctuations and the signals from external forcings of the climate system, were not separated in this study. This means that it is impossible to trace the origin of the EASM decadal shift from the present study alone. The roles of anthropogenic aerosols (e.g., black carbon and sulfates) and greenhouse gases in modulating the EASM decadal shift cannot be ignored (e.g., Xu, 2001; Menon et al., 2002; Lau and Kim, 2006; Zhao et al., 2006). Although precipitation is the most important variable for measuring the EASM, the precipitation shift in the present model results does not match the observation data well. Nevertheless, further studies are needed to address these issues.

Acknowledgements. This research was jointly supported by the National Basic Research Program of China, "Structures, Variability and Climatic Impacts of Ocean Circulation and Warm Pool in the Tropical Pacific Ocean" (Grant No. 2012CB417403), the National Science Foundation of China under grant 41205048 and the special projects of China Meteorological Administration on public interests (Grant No. GYHY201006022).

REFERENCES

Chen, X., S. Li, and G. Li, 2010: Opposite impact of tropical Indian Ocean and Pacific Ocean warming on the East Asian summer monsoon. *Transactions of Atmospheric Sciences*, **33**(5), 624–633. (in Chinese)

Ding, T., Y. Sun, Z. Wang, Y. Zhu, and Y. Song, 2009: Inter-decadal variation of the summer precipitaiton in China and its association with decreasing Asian summer monsoon. Part II: Possible causes. *Int. J. Climatol.*, **29**, 1920–1944, doi: 1.1002/joc.1759.

Ding, Y., Z. Wang, and Y. Sun, 2008: Inter-decadal variation of the summer precipitation in East China and its association with decreasing Asian summer monsoon. Part I: Observed evidences. *Int. J. Climatol.*, **28**, 1139–1161, doi: 10.1002/joc.1615.

Fu, J., S. Li, and D. Luo, 2009: Impact of global SST on decadal shift of East Asian summer climate. *Adv. Atmos. Sci.*, **26**, 192–201, doi: 10.1007/s00376-009-0192-z.

Fu, J., and S. Li, 2012: Intercomparison of the South Asian High in the three reanalyses, NCEP1, NCEP2, and ERA40 and in the station observation. *Atmos. Oceanic Sci. Lett.*, **5**(3), 189–194.

GAMT (the GFDL global Atmospheric Model development Team), 2004: The new GFDL Atmosphere and Land Model AM2-LM2: Evaluation with prescribed SST simulations. *J. Climate*, **17**, 4641–4673.

Gong, D., and C. Ho, 2002: Shift in the summer rainfall over the Yangtze River valley in the late 1970s. *Geophys. Res. Lett.*, **29**(10), 1436, doi: 10.1029/2001GL014523.

Han, J., and H. Wang, 2007: Interdecadal variability of East Asian summer monsoon in an AGCM model. *Adv. Atmos. Sci.*, **24**(5), 808–818, doi: 10.1007/s00376-007-0808-0.

Hoerling, M., J. Hurrell, T. Xu, G. Bates, and A. Phillips, 2004: Twentieth century North Atlantic climate change. Part II: Understanding the effect of Indian Ocean warming. *Climate Dyn.*, **23**, 391–405.

Hu, Z., 1997: Interdecadal variability of summer climate

over East Asia and its association with 500 hPa height and global sea surface temperature. *J. Geophys. Res.*, **102**, 19403–19412.

Huang, R., 2001: Decadal variability of the summer monsoon rainfall in East Asia and its association with the SST anomalies in the tropical Pacific. *CLIVAR Exchange*, **2**, 7–8.

Kalnay, E., and Coauthors, 1996: The NCEP/NCAR 40-year reanalysis project. *Bull. Amer. Meteor. Soc.*, **77**, 437–471.

Lau, K.-M, and M. T. Li, 1984: The monsoon of east Asia and its global association. *Bull. Amer. Meteor. Soc.*, **65**, 114–125.

Lau, K.-M., and M. Kim, 2006: Observational relationships between aerosol and Asian monsoon rainfall and circulation. *Geophys. Res. Lett.*, **33**, L21810. doi: 10.1029/2006GL027546.

Li, H., A. Dai, T. Zhou, and J. Lu, 2008a: Responses of East Asian summer monsoon to historical SST and atmospheric forcing during 1950–2000. *Climate Dyn.*, doi: 10.1007/s00383-008-0482-7.

Li, S., J. Lu, G. Huang, and K. Hu, 2008b: Tropical Indian Ocean warming East Asian summer monsoon: A multiple AGCM study. *J. Climate*, **21**, 6080–6088.

Lu, R., 2002: Indices of the summertime western North Pacific subtropical high. *Adv. Atmos. Sci.,* **19**(6), 1004–1028.

Menon, S., J. Hansen, L. Nazarenko, and Y. Luo, 2002: Climate effects of black carbon aerosols in China and India. *Science*, **297**, 2250–2253.

Mitchell, T., and P. Jones, 2005: An improved method of constructing a database monthly climate observations and associated high-resolution grids. *Int. J. Climatol.,* **25**, 693–712.

Rayner, N., E. Horton, D. parker, C. Folland, and R. Hackett, 1996: Version 2.2 of the Global Sea-Ice and Sea Surface Temperature Data Set, 1903–1994. Climate Research Technical Note 74, Hadley Center for Climate Prediction and Research, UK Meteorological Office.

Renwick, J., 2002: Southern Hemispheric circulation and relations with sea ice and sea surface temperatures. *J. Climate*, **15**, 3058–3068.

Si, D., Y. Ding, and Y. Liu, 2009: Decadal northward shift of the Meiyu belt and the possible cause. *Chinese Science Bulletin*, **54**, 4742–4748, doi: 10.1007/s11434-009.

Upplal, S., and Coauthors, 2004: ERA-40: ECMWF 45-years reanalysis of the global atmosphere and surface conditions 1957–2001. *ECMWF Newsletter Meteorology*, **101**, 2–21.

Wang, H., 2001: The weakening of the Asian monsoon circulation after the end of 1970s. *Adv. Atmos. Sci.*, **18**, 376–386.

Webster, P., and S. Yang, 1992: Monsoon and ENSO: Selectively interactive systems. *Quart. J. Roy. Meteor. Soc.*, **118**, 877–926.

Xie, P., and P. A. Arkin, 1996: Analyses of global monthly precipitation using gauge observations, satellite estimates, and numerical model predictions. *J. Climate*, **9**, 840–858.

Xu, Q., 2001: Abrupt change of the mid-summer climate in central east China by the influence of atmospheric pollution. *Atmos. Environ.*, **35**, 5029–5040.

Yang, J., Q. Liu, S. Xie, Z. Liu, and L. Wu, 2007: Impact of the Indian Ocean SST basin mode on the Asian summer monsoon. *Geophys. Res. Lett.*, **34**, L02708, doi: 10.1029/2006GL028571.

Yang, S., and K.-M. Lau, 1998: Influences of sea surface temperature and ground wetness on Asian summer monsoon. *J. Climate*, **11**, 3230–3246.

Zeng, G., Z. Sun, W. Wang, Z. Lin, and D. Ni, 2007: Interdecadal variation of East Asian summer monsoon—Simulated by NCAR Cam3 driven by global SSTs. *Climatic and Environmental Research*, **12**(2), 211–224. (in Chinese)

Zeng, G., Z. Sun, Z. Lin, and D. Ni, 2010: Numerical simulation of impacts of sea surface temperature anomaly upon the interdecadal variation in the northwestern Pacific subtropical high. *Chinese J. Atmos. Sci.*, **34**(2), 307–322. (in Chinese)

Zhang, Q., Y. Qian, and X. Zhang, 2000: Interannual and Interdecadal variations of the south Asian high. *Chinese J. Atmos. Sci.*, **24**(1), 67–78. (in Chinese)

Zhang, Q., J. Lu, L. Yang, J. Wei, and J. Peng, 2007: The interdecadal variation of precipitation pattern over China during summer and its relationship with the atmospheric internal dynamic processes and extra-forcing factors. *Chinese J. Atmos. Sci.*, **31**(6), 1290–1300. (in Chinese)

Zhang, Y., J. Wallace, and D. Battisti, 1997: ENSO-like interdecadal variability: 1900–93. *J. Climate*, **10**, 1004–1020.

Zhao, C., X. Tie, and Y. Lin, 2006: A possible positive feedback of reduction of precipitation and increase in aerosols over eastern central China. *Geophys. Res. Lett.*, **33**, L11814, doi: 10.1029/2006GL025959.

Zhou, T., and Coauthors, 2009: Why the western Pacific subtropical high has extended westward since the late 1970s. *J. Climate*, **22**, 2199–2215.

Zhu, Y., H. Wang, W. Zhou, and J. Ma, 2010: Recent changes in the summer precipitation pattern in East China and the background circulation. *Climate Dyn.*, **36**, 1463–1473, doi: 10.1007/s00382-010-0852-9.